Effects of added inulin and wheat gluten on structure of rye porridge

José L. Vázquez-Gutiérrez*, Daniel Johansson, Maud Langton

Department of Food Science, SLU - Swedish University of Agricultural Sciences, PO Box 7051, SE-750 07 Uppsala, Sweden

* Corresponding author. Department of Food Science, SLU - Swedish University of Agricultural Sciences, PO Box 7051, SE-750 07 Uppsala, Sweden. Tel.: +46 (0)18-671983. Email address: jose.luis.vazquez.gutierrez@slu.se (J.L. Vázquez-Gutiérrez).

Abstract

The aim was to study the microstructure and distribution of components of rye porridge enriched with different inulin and gluten proportions (0:0, 3:9, 6:6, 9:3), and their relationship with texture. Inulin was labeled with fluorescein isothiocyanate (FITC) prior to its addition to the porridges, and multiple staining was applied to cryosections in order to also observe other components of the porridges. Porridge structure consisted of grain fragments and a continuous phase formed by released amylose, starch granules and protein. Addition of inulin and gluten to rye porridge partly hindered starch gelatinization due to their water binding capacity. The green fluorescence from FITC-labeled inulin was brighter in detached starch granules in the continuous phase, indicating greater interaction of inulin with starch than with protein. Viscosity was lower in those porridges with high

inulin content and low gluten content. Solubilized inulin created a protective layer around starch granules limiting their swelling and amylose release, which may explain the differences in viscosity between the porridges and could have further influence in starch digestibility.

Highlights

- Addition of inulin and gluten affected microstructure and texture of rye porridge
- FITC labeling allowed localizing solubilized inulin in the porridge
- Inulin accumulated preferentially around starch granules hindering their swelling
- Starch digestibility could be affected by the addition of inulin and gluten

Keywords: rye, starch, microscopy, fructan, viscosity

1. Introduction

Consumers are demanding healthier food products with improved functionalities and an increasing number of new food formulations are being developed to satisfy this need. The compatibility or incompatibility between ingredients in new food formulations can affect both texture and structure (Icoz, Moraru, & Kokini, 2005). These structural changes could also have later implications in the intended functionality of the product (McClements, Decker, Park, & Weiss, 2009). When it comes to porridge, the rheological properties are of great importance for quality control and consumer acceptance (Sai Manohar, Urmila Devi, Bhattacharya, & Venkateswara Rao, 2011). Moreover, it can also have influence on the satiating properties of the product (Mars, Hogenkamp, Gosses, Stafleu, & De Graaf, 2009). Rye foods, which are important elements in the healthy Nordic diet, have shown favorable effects on appetite (Isaksson et al., 2012), as well as beneficial effects on postprandial insulin responses and inflammatory biomarkers (Fung et al., 2002; Landberg et al., 2010; Rosén, Östman, & Björck, 2011). Addition of plant protein and fermentable dietary fiber could possibly enhance the appetite suppressing effect of whole-grain rye porridge. Such effects may in part be due to alterations in the microstructure of the product (Lundin, Golding, & Wooster, 2008).

Inulin is an oligo-fructose polymer of interest in human nutrition due to its ability to act as dietary fiber and prebiotic (Roberfroid, 2007). Due to its structure, inulin resists digestion in the human intestine and is fermented by bacteria in the colon, which has been suggested to affect appetite (Cani, Dewever, & Delzenne, 2004). Little work has been done to investigate the effects of inulin on food structure. Microstructural studies of inulin-enriched products have been carried out on cereal and dairy products (Aravind, Sissons, Fellows, Blazek, & Gilbert, 2012; Guardeño, Vázquez-Gutiérrez, Hernando, & Quiles, 2013; Guggisberg,

Cuthbert-Steven, Piccinali, Bütikofer, & Eberhard, 2009; Rodríguez-García, Puig, Salvador, & Hernando, 2012; Sołowiej et al., 2015). However, the studies do not provide a detailed localization of solubilized inulin in the structure and only insolubilized inulin crystals have been detected by light microscopy (Guardeño et al., 2013). Interactions between inulin and the protein structural network in yogurt have been suggested (Guggisberg et al., 2009; Kip, Meyer, & Jellema, 2006), but such interactions have neither been properly described nor confirmed by microstructural observations.

Gluten is found in the endosperm of cereals such as wheat, barley, and rye and is an important by-product from wet milling of wheat flour. Wheat gluten is a common food ingredient in bakery products such as hamburger buns (Esteller, Pitombo, & Lannes, 2005), meat products as binding and enriching ingredient (Zhang, Xiao, Samaraweera, Lee, & Ahn, 2010), breakfast cereals, and pasta (Day, 2011). Wheat gluten is marketed in two forms: 'nonvital' and 'vital'. Nonvital wheat gluten has undergone irreversible denaturation, while vital dry gluten in contact with water rehydrates rapidly and regains its intrinsic functionality (Esteller et al., 2005). Therefore, vital gluten constitutes a desired additive in baked and meat products due to its ability to form a viscoelastic mass through the interaction with water (Esteller et al., 2005; Zhang et al., 2010). Interactions between gluten and starch have been reported and supported by microscopy observation (Chen, Deng, Wu, Tian, & Xie, 2010). It has also been suggested that there could be interactions between gluten and inulin but this has not been confirmed by microstructural observation (Morris & Morris, 2012; Peressini & Sensidoni, 2009; Rubel, Pérez, Manrique, & Genovese, 2015; Wang, Rosell, & Benedito de Barber, 2002).

Labeling of inulin with fluorescein isothiocyanate (FITC) has been successfully used for studies of the phase behavior of inulin-waxy maize starch systems (Zimeri & Kokini, 2003a).

To our knowledge, the method has so far only been used for model systems and this is the first time that FITC labeling and localization of inulin by confocal microscopy is performed in a complex food system. Previously only inulin crystals could be identified and the location of soluble inulin could only be suggested in such systems, not proven by fluorescence signal as in this study.

The aim of this study was to analyze the effect of partial substitution of rye flakes for inulin and gluten on the microstructure and texture of whole grain rye flake porridge to obtain a better understanding of the functionality of the product.

2. Materials and Methods

2.1. Sample preparation

Rye porridge was made from whole grain rye flakes, produced by steaming, cutting and rolling rye kernels (Lantmännen Cerealia, Järna, Sweden). Four different samples were prepared, one with 40 g rye flakes and the rest contained 40 g rye flakes with different combinations of inulin (Orafti®GR inulin, purity 90%; Beneo, Mannheim, Germany) and gluten (Vital Wheat Gluten, purity 77%; Arrowhead Mills, Boulder, USA). The combined additions were recalculated to compensate for impurities to ensure ratios inulin/gluten of 1:3 (3 g inulin and 9 g gluten, 3I9G), 1:1 (6 g inulin and 6 g gluten, 6I6G) and 3:1 (9 g inulin and 3 g gluten, 9I3G), as well as similar total weight of all the porridges. Samples were prepared by adding boiling water (150 g) to the rye flakes/inulin/gluten mixtures and manually stirred for 30 sec. The samples were then left to rest for 2 min and manually stirred again for another 30 sec. The samples were left to rest for another 2 min, and then deposited in aluminum caps and frozen with liquid nitrogen. Short-chain inulin (degree of polymerization between 10 and 20) was chosen as it would have greater solubility than

long-chain inulin (Tárrega, Torres, & Costell, 2011) and would be expected to have less effect on the viscosity of the product (Morris & Morris, 2012; Tárrega et al., 2011).

2.2. Labeling method

Inulin was covalently labeled with fluorescein isothiocyanate (FITC, Sigma-Aldrich Co. LLC., St Louis, MO) following the procedure described by Zimeri and Kokini (2003a) with modifications. Briefly, inulin (1g) was dissolved in dimethyl sulfoxide (10 mL) containing two drops of pyridine. FITC (0.04 g) was added, followed by addition of the catalyst dibutylin dilaurate (20 mg). The mixture was heated for 3 h at 50 °C using a water bath. Several precipitations in ethanol were performed to remove the free dye. FITC-inulin was filtered using a filter paper No. 3 (Whatman, Wand R Balston Ltd, England), dried overnight in a vacuum oven at 85 °C, and stored in the dark under refrigeration to prevent loss of fluorescence. In order to prepare the porridges, an amount of FITC-labeled inulin (1% of the total inulin amounts described in section 2.1) was added before the mixing with hot water and the sample preparation procedure outlined in section 2.1 was followed.

2.3. Microscopy

The frozen samples were transferred to a cryostat, and 8 μm cryosections were obtained and placed in glass slides. Multiple staining was applied to cryosections, lugol's solution (0.05 g/L iodine) to detect starch and protein (Groves, 2006), 0.1 g/L Calcofluor White for β-glucan (Dornez et al., 2011), and 0.02 g/L Texas Red for protein (Johansson, Krona, & Stading, 2012). A Nikon Eclipse Ni-U research microscope coupled to a HGFI mercury lamp (Nikon, Tokyo, Japan) was used to visualize the microstructure of the porridges. Bright field and epifluorescence images were obtained using CFI Plan 4X objective (N.A. 0.20, W.D. 20

mm) and CFI Plan Fluor 10X (N.A. 0.30, W.D. 16 mm) and 20X (N.A. 0.75, W.D. 1 mm) objectives. Blue (Epi-FL Filterset DAPI, excitation wavelength 382-393 nm, emission 417-477), green (Epi-FL Filterset FITC, excitation wavelength 465-500 nm, emission 516-556 nm), and red (Epi-FL Filterset Texas Red, excitation 540-580 nm, emission 600-660 nm) light fluorescence filters were used to observe the fluorescence of Calcofluor, FITC-inulin, and Texas Red, respectively. Images were captured with a Nikon Digital Sight DS-Fi2-U3 digital camera.

2.4. Texture analysis

A RVA (Rapid Visco Analyzer, Newport Scientific Pvt. Ltd., Australia) with an impeller-cup combination was used to measure the viscosity of the porridges. Since rye porridge includes particles in the millimeter range it is impossible to use rheometry with gap distances which would give controlled shear rates and absolute measurements. For the RVA measurement the average temperature, as measured with a thermocouple connected to a digital readout during the preparation process described in section 2.1, was used. The rate profile was set to simulate the stirring with an extra measurement period at the end of the run (Table 1). For each different formulation, approximately 35 g of the sample were introduced in a stainless steel cylinder and analyzed in the RVA in triplicate. The average viscosity during the last 15 s of each measurement period was used to derive a viscosity profile for each product. The first 15 s of the measurement periods were not included to avoid the initial instabilities.

Table 1

155 **2.5. Statistical analysis**

156 Differences between viscosity profiles were evaluated using a mixed effect model suitable
157 for repeated measurements with PROC mixed in SAS, version 9.4 (SAS Institute Inc, Cary, NC,
158 USA). Time, product and a time x product interaction term were included as fixed effects
159 with time as a repeated variable. Sample was included as a random effect. When a
160 significant time x product interaction was found, Tukey's honest significance test was
161 performed for each time point.

162

163 **3. Results and discussion**

164 **3.1. Characterization of porridge structure by iodine staining**

165 After the addition of hot water to the whole grain rye flakes, starch granules swelled and
166 collapsed leading to gelatinization. The structure of the rye porridges, as visualized with
167 iodine staining, consisted of kernel fragments and an aqueous continuous phase with
168 released amylose (blue) and amylopectin (brown/purple), small fragments of starch
169 granules (dark blue/violet) and protein (yellow). Iodine staining, further allowed for
170 visualization of the aleurone and subaleurone cells, both rich in protein, as shown in yellow
171 color (Fig. 1A and B). Amylose and amylopectin seen in the continuous phase were released
172 from starch granules at the edge of the grain fragments as these had more access to water
173 and therefore underwent greater swelling. A few detached starch granules could be
174 distinguished in the aqueous phase, showing great level of distortion (Fig. 1C).
175 Starch granules in porridges containing inulin and gluten appeared to be less swollen than
176 the ones in the control product (Fig. 1D-F). This may be due to inulin and gluten competing
177 for water against the starch, owing to their water binding capacity, as has previously been
178 suggested in white sauces formulated with soy protein and inulin (Guardeño et al., 2013).

With no inulin and gluten added, more water was available for the starch, leading to greater swelling of the granules.

The porridge with the highest amount of inulin (9I3G) showed smaller and less distorted starch granules in the continuous phase compared with the sample with the highest amount of gluten (3I9G). Moreover, the 9I3G presented less amount of released amylose/amylopectin in the aqueous phase, which appeared less stained than in the other samples.

According to Bishay (1998) and Manno et al. (2009), inulin has a greater affinity for the water than starch polysaccharides and gluten. The water that is bound to inulin chains is more mobile than when it is bound to the starch; this is simply due to inulin having shorter, more mobile molecules (Lobato, Grossmann, & Benassi, 2009). The inulin's preferential properties for hydrating, aggregating, and forming a matrix encase starch granules in a semi-solid gel (Tolstoguzov, 2003). This encasing of the starch granules would possibly limit water movement to the starch granules, reducing swelling and gelatinization (Brennan et al., 2004).

Fig. 1

3.2. Location of inulin by epifluorescence

When samples were observed under epifluorescence, inulin labeled with FITC could be detected as green fluorescence. The control sample, which did not contain inulin, presented faint green autofluorescence from proteins and cell walls (Fig. 2A). However, strong green autofluorescence was detected in the pericarp due to the high concentration of phenolic acids in that area (Dornez et al., 2011). Therefore, the pericarp area appeared in light blue-

turquoise color in all the samples after combining blue and green fluorescence signals (Fig. 2A-D). Calcofluor staining allowed detecting β-glucan as blue fluorescence. High concentration of β-glucan was observed in the aleurone and subaleurone layers, where thick and relatively intact cell walls were observed. The blue fluorescence lost continuity and became thinner towards deeper layers of the starch endosperm, indicating that cell walls were damaged and β-glucan content was lower in those areas (Fig. 2A). Fragments of cell walls with β-glucan could also be found in the aqueous phase among detached starch granules and protein aggregates (Fig. 2B-D).

Green fluorescence signal from FITC-labeled inulin was observed heterogeneously distributed in the aqueous phase and it was brighter as the amount of added inulin increased. In the sample with lower amount of added inulin (3I9G), the green fluorescence appeared to be slightly brighter in specific areas (Fig. 2B). These areas were stained in black-dark blue color after lugol staining (Fig. 2F), corresponding to non-gelatinized starch granules and aggregates of released amylose. In the samples with equal amount of added inulin and gluten (6I6G), the fluorescence from the amylose aggregates became brighter (Fig. 2C). Bright green fluorescence could also be observed around the gluten aggregates, which were stained in yellow with lugol (Fig. 2G), which could indicate interactions between inulin and gluten protein. The formulation with the highest amount of inulin (9I3G) presented the brightest green fluorescence overall, especially located in the starchy areas rich in amylose (Fig. 2D and H).

Some studies have not found evidence of interaction between inulin and amylopectin (Icoz & Kokini, 2008; Zimeri & Kokini, 2003b). Therefore, it was concluded that the green fluorescence observed in the starchy areas was due to interaction between inulin and amylose or with starch granule-associated proteins.

Fig. 2

When samples were observed at higher magnification, bluish precipitates could be observed around gluten aggregates after iodine staining in the porridges with medium and high amount of inulin (6I6G and 9I3G), as shown in Fig. 3A. These precipitates could correspond to released amylose, which would be interacting with the gluten protein. In the same way, bright green fluorescence surrounding the gluten aggregates, which could be detected as red fluorescence after Texas Red staining, could be observed (Fig. 3B). This indicated the presence of inulin in similar areas where the amylose was located. Both amylose and inulin could interact with gluten protein.

Fig. 3

3.3. Texture analysis

A statistically significant interaction between product x time was detected on the viscosity profiles ($P<0.05$). Therefore, Tukey's honest significance test was performed for each time-point. All porridges exhibited increasing viscosity during the measurement (Figure 4). This increase in viscosity was likely due to a series of changes taking place in the structure of the porridges. The starch granules swell and amylose and amylopectin leach from the granules resulting in increased viscosity. Simultaneously, granules rapture and amylose and amylopectin chains align, contributing to decreased viscosity. Among the enriched porridges, the final viscosity values significantly decreased ($P<0.05$) with increasing inulin

content and decreasing gluten content (Figure 4). A similar trend was also seen at the two first time points. Since the enriched porridges contained higher amount of dry matter compared to the control porridge (more than 52 g for the enriched versus 40 g for the control), all the enriched porridges would be expected to have higher viscosity values. However, all enriched porridges, except the porridge with highest gluten content (3I9G), had significantly lower ($P<0.05$) viscosity than the control one at all time points.

Fig. 4

The high water binding capacity of inulin and gluten decrease the water available for starch gelatinization. Moreover, as observed in the microstructural study, inulin was located preferentially around detached starch granules. The significantly lower ($P<0.05$) final viscosity measured in the samples with higher inulin content (9I3G and 6I6G) could also be due to the additional effect of inulin, encasing the starch granules, as observed in the epifluorescence images (Fig. 2B-D). This would limit the release of amylose from the granules and result in a smaller contribution from the starch network to the viscosity. Gluten aggregates could also interfere with the starch network thereby decreasing the viscosity. Chen et al. (2010) reported that type and amount of added gluten had considerable influence on the mechanisms involved in the pasting properties of starch, such as transportation of available water and transmission of gelatinization energy. However, since the viscosity reached in the porridges decreased with increasing inulin content, it seems that inulin had greater influence on the viscosity of the porridge than gluten (Figure 4). Moreover, as shown in the microstructural study, gluten occurs as bigger particles while inulin seems to accumulate at surfaces with amylose. The higher content of particles in the

275 porridge with the highest gluten content could contribute to the increase in viscosity and
276 would explain the differences in viscosity observed between the porridges.
277 Unlike what has been previously reported in white sauces (Guardeño, Hernando, Llorca,
278 Hernández-Carrión, & Quiles, 2012; Guardeño et al., 2013), no signs of inulin insolubility or
279 recrystallization could be observed in porridges. Kim, Faqih, and Wang (2001) reported that
280 low concentrations of inulin such as 0.5 g/L do not lead to gel network formation after
281 heating at 80 °C. The concentration of inulin in the porridge with highest inulin content
282 (9I3G) was 0.67 g/L. According to Kim et al. (2001), approximately 2.5 g/L inulin can be
283 dissolved at 80 °C. Furthermore, short-chain inulin, as the one used in this study, is more
284 likely to remain solubilized than long-chain inulin (Tárrega et al., 2011). Therefore, it could
285 be concluded that inulin was completely dissolved in all the porridges and that
286 concentration was not sufficient for gel formation.
287 The protective effect of inulin on starch granules to reduce swelling and resist degradation
288 has previously been reported for inulin-enriched white sauces, leading to a less compact and
289 cohesive continuous phase (Guardeño et al., 2012; Guardeño et al., 2013). Since the
290 concentration of inulin reached in the porridges was relatively low, the density of inulin
291 chains would not be able to reach a critical crowding effect. Therefore, inulin would act as
292 diluent in the porridges without interacting synergistically with starch, as has been reported
293 for mashed potato (Alvarez, Fernández, Solas, & Canet, 2011). Contrarily, other studies on
294 inulin-enriched products, such as yoghurt, have reported a marked increase in the
295 consistency with the addition of inulin, which has been attributed to the generation of a
296 second network supporting the one of casein (Guggisberg et al., 2009). Kip et al. (2006)
297 concluded that inulin may also be partially involved in the formation of the protein
298 structural network during yoghurt fermentation by complexation with protein aggregates.

Differential scanning calorimetry analyses on potato starch-inulin gels have also suggested that gelatinization of potato starch with inulin produced binary gel of common network that could result from the competition of both components for water (Krystyjan, Ciesielski, Khachatryan, Sikora, & Tomasik, 2015). Aravind et al. (2012) hypothesized that relatively small amounts of inulin, similar to those added to rye porridge in this study, support formation of a well-developed protein–fiber matrix subsequently acting as a physical barrier to starch-degrading enzymes based on *in vitro* starch digestion tests. In this way, the addition of inulin to rye porridge could limit starch digestibility and have later implications for the glycemic response. Consequently it could potentially be utilized for the development of products with reduced glycemic index.

4. Conclusions

Addition of inulin and gluten to rye porridge partly hindered starch gelatinization due to their water binding capacity. Inulin was completely solubilized and preferentially located in detached starch granules of the aqueous phase of the porridge, which could be due to interaction between inulin and amylose molecules. The solubilized inulin would create a protective layer around the starch granules limiting their swelling and the amylose release. This protective matrix around the starch granules, together with the water binding capacity of inulin and gluten, would explain the lower viscosity values observed in the porridges with added inulin and gluten. On the other hand, the presence of gluten particles would contribute to increased viscosity and could explain the higher viscosity observed for the porridge with highest gluten content compared to the other enriched porridges. This feature may lead to limited accessibility of starch-degrading enzymes, which could affect starch digestibility *in vivo* and glycemic index.

Acknowledgements

The authors thank Dr. Rikard Landberg for discussions and comments related to the current work, Isabella Lee for her input on ingredients and sample preparation, and Lantmännen for providing the products for the study.

References

Alvarez, M. D., Fernández, C., Solas, M. T., & Canet, W. (2011). Viscoelasticity and microstructure of inulin-enriched mashed potatoes: Influence of freezing and cryoprotectants. *Journal of Food Engineering, 102*, 66-76.

Aravind, N., Sissons, M. J., Fellows, C. M., Blazek, J., & Gilbert, E. P. (2012). Effect of inulin soluble dietary fibre addition on technological, sensory, and structural properties of durum wheat spaghetti. *Food Chemistry, 132*, 993-1002.

Cani, P. D., Dewever, C., & Delzenne, N. M. (2004). Inulin-type fructans modulate gastrointestinal peptides involved in appetite regulation (glucagon-like peptide-1 and ghrelin) in rats. *Br J Nutr, 92*, 521-526.

Chen, J.-s., Deng, Z.-y., Wu, P., Tian, J.-c., & Xie, Q.-g. (2010). Effect of gluten on pasting properties of wheat starch. *Agricultural Sciences in China, 9*, 1836-1844.

Day, L. (2011). Wheat gluten: production, properties and application. In G. O. Phillips & P. A. Williams (Eds.), *Handbook of Food Proteins* (pp. 267-288): Woodhead Publishing.

Dornez, E., Holopainen, U., Cuyvers, S., Poutanen, K., Delcour, J. A., Courtin, C. M., & Nordlund, E. (2011). Study of grain cell wall structures by microscopic analysis with four different staining techniques. *Journal of Cereal Science, 54*, 363-373.

347 Esteller, M. S., Pitombo, R. N. M., & Lannes, S. C. S. (2005). Effect of freeze-dried gluten addition on
348 texture of hamburger buns. *Journal of Cereal Science, 41*, 19-21.
349 Fung, T. T., Hu, F. B., Pereira, M. A., Liu, S., Stampfer, M. J., Colditz, G. A., & Willett, W. C. (2002).
350 Whole-grain intake and the risk of type 2 diabetes: a prospective study in men. *The*
351 *American Journal of Clinical Nutrition, 76*, 535-540.
352 Groves, K. (2006). Microscopy: a tool to study ingredient interactions in foods. In A. G. Gaonkar & A.
353 McPherson (Eds.), *Ingredient interactions: effects on food quality*. Boca Raton: CRC Press.
354 Guardeño, L. M., Hernando, I., Llorca, E., Hernández-Carrión, M., & Quiles, A. (2012).
355 Microstructural, physical, and sensory impact of starch, inulin, and soy protein in low-fat
356 gluten and lactose free white sauces. *Journal of Food Science, 77*, C859-C865.
357 Guardeño, L. M., Vázquez-Gutiérrez, J. L., Hernando, I., & Quiles, A. (2013). Effect of different rice
358 starches, inulin, and soy protein on microstructural, physical, and sensory properties of low-
359 fat, gluten, and lactose free white sauces. *Czech Journal of Food Sciences, 31*, 575-580.
360 Guggisberg, D., Cuthbert-Steven, J., Piccinali, P., Bütikofer, U., & Eberhard, P. (2009). Rheological,
361 microstructural and sensory characterization of low-fat and whole milk set yoghurt as
362 influenced by inulin addition. *International Dairy Journal, 19*, 107-115.
363 Icoz, D. Z., & Kokini, J. L. (2008). Theoretical analysis of predictive miscibility of carbohydrate
364 polymers – Software calculations for inulin–amylopectin systems. *Carbohydrate Polymers,*
365 *72*, 52-59.
366 Icoz, D. Z., Moraru, C. I., & Kokini, J. L. (2005). Polymer–polymer interactions in dextran systems
367 using thermal analysis. *Carbohydrate Polymers, 62*, 120-129.
368 Isaksson, H., Tillander, I., Andersson, R., Olsson, J., Fredriksson, H., Webb, D.-L., & Åman, P. (2012).
369 Whole grain rye breakfast — Sustained satiety during three weeks of regular consumption.
370 *Physiology & Behavior, 105*, 877-884.

Johansson, D., Krona, A., & Stading, M. (2012). Influence of surface lipids in commercial zein on microstructure and rheological properties of gluten-free dough. *Annual Transactions of the Nordic Rheology Society, 20*, 247-251.

Kim, Y., Faqih, M. N., & Wang, S. S. (2001). Factors affecting gel formation of inulin. *Carbohydrate Polymers, 46*, 135-145.

Kip, P., Meyer, D., & Jellema, R. H. (2006). Inulins improve sensoric and textural properties of low-fat yoghurts. *International Dairy Journal, 16*, 1098-1103.

Krystyjan, M., Ciesielski, W., Khachatryan, G., Sikora, M., & Tomasik, P. (2015). Structure, rheological, textural and thermal properties of potato starch – Inulin gels. *LWT - Food Science and Technology, 60*, 131-136.

Landberg, R., Andersson, S.-O., Zhang, J.-X., Johansson, J.-E., Stenman, U.-H., Adlercreutz, H., . . . Hallmans, G. (2010). Rye whole grain and bran intake compared with refined wheat decreases urinary C-peptide, plasma insulin, and prostate specific antigen in men with prostate cancer. *The Journal of Nutrition, 140*, 2180-2186.

Lobato, L. P., Grossmann, M. V. E., & Benassi, M. T. (2009). Inulin addition in starch-based dairy desserts: Instrumental texture and sensory aspects. *Food Science and Technology International, 15*, 317-323.

Lundin, L., Golding, M., & Wooster, T. J. (2008). Understanding food structure and function in developing food for appetite control. *Nutrition & Dietetics, 65*, S79-S85.

Manno, D., Filippo, E., Serra, A., Negro, C., De Bellis, L., & Miceli, A. (2009). The influence of inulin addition on the morphological and structural properties of durum wheat pasta. *International Journal of Food Science & Technology, 44*, 2218-2224.

Mars, M., Hogenkamp, P. S., Gosses, A. M., Stafleu, A., & De Graaf, C. (2009). Effect of viscosity on learned satiation. *Physiology & Behavior, 98*, 60-66.

McClements, D. J., Decker, E. A., Park, Y., & Weiss, J. (2009). Structural design principles for delivery of bioactive components in nutraceuticals and functional foods. *Critical Reviews in Food Science and Nutrition, 49*, 577-606.

Morris, C., & Morris, G. A. (2012). The effect of inulin and fructo-oligosaccharide supplementation on the textural, rheological and sensory properties of bread and their role in weight management: A review. *Food Chemistry, 133*, 237-248.

Peressini, D., & Sensidoni, A. (2009). Effect of soluble dietary fibre addition on rheological and breadmaking properties of wheat doughs. *Journal of Cereal Science, 49*, 190-201.

Roberfroid, M. B. (2007). Inulin-type fructans: functional food ingredients. *The Journal of Nutrition, 137*, 2493S-2502S.

Rodríguez-García, J., Puig, A., Salvador, A., & Hernando, I. (2012). Optimization of a sponge cake formulation with inulin as fat replacer: structure, physicochemical, and sensory properties. *Journal of Food Science, 77*, C189-C197.

Rosén, L. A. H., Östman, E. M., & Björck, I. M. E. (2011). Effects of cereal breakfasts on postprandial glucose, appetite regulation and voluntary energy intake at a subsequent standardized lunch; focusing on rye products. *Nutrition Journal, 10*, 7-7.

Rubel, I. A., Pérez, E. E., Manrique, G. D., & Genovese, D. B. (2015). Fibre enrichment of wheat bread with Jerusalem artichoke inulin: Effect on dough rheology and bread quality. *Food Structure, 3*, 21-29.

Sai Manohar, R., Urmila Devi, G. R., Bhattacharya, S., & Venkateswara Rao, G. (2011). Wheat porridge with soy protein isolate and skimmed milk powder: Rheological, pasting and sensory characteristics. *Journal of Food Engineering, 103*, 1-8.

Sołowiej, B., Glibowski, P., Muszyński, S., Wydrych, J., Gawron, A., & Jeliński, T. (2015). The effect of fat replacement by inulin on the physicochemical properties and microstructure of acid casein processed cheese analogues with added whey protein polymers. *Food Hydrocolloids, 44*, 1-11.

421 Tárrega, A., Torres, J. D., & Costell, E. (2011). Influence of the chain-length distribution of inulin on
422 the rheology and microstructure of prebiotic dairy desserts. *Journal of Food Engineering,*
423 *104*, 356-363.
424 Wang, J., Rosell, C. M., & Benedito de Barber, C. (2002). Effect of the addition of different fibres on
425 wheat dough performance and bread quality. *Food Chemistry, 79*, 221-226.
426 Zhang, W., Xiao, S., Samaraweera, H., Lee, E. J., & Ahn, D. U. (2010). Improving functional value of
427 meat products. *Meat Science, 86*, 15-31.
428 Zimeri, J. E., & Kokini, J. L. (2003a). Morphological characterization of the phase behavior of inulin–
429 waxy maize starch systems in high moisture environments. *Carbohydrate Polymers, 52*, 225-
430 236.
431 Zimeri, J. E., & Kokini, J. L. (2003b). Phase transitions of inulin–waxy maize starch systems in limited
432 moisture environments. *Carbohydrate Polymers, 51*, 183-190.

Figure captions

Fig. 1. Light microscopy images of different porridge cryosections stained with lugol's solution. A-C) Control; D) 3:9 inulin/gluten (3I9G); E) 6:6 inulin/gluten (6I6G); F) 9:3 inulin/gluten (9I3G). gf: grain fragment; al: aleurone; ap: aqueous phase.

Figure 2. Microstructure of porridge with different inulin and gluten proportions: 0:0 (control), 3:9 (3I9G), 6:6 (6I6G), 9:3 (9I3G). Epifluorescence images (top row) with Calcofluor White staining (blue fluorescence for β-glucan and green fluorescence for FITC-labeled inulin) and bright field images (bottom row) with iodine staining (protein in yellow, amylose in blue, amylopectin in purple). Red arrows: inulin rich areas (top row) colocalized with starch areas (bottom row). Same areas are shown in both rows.

Fig. 3. Microstructure of rye porridge with equal amounts of added gluten and inulin (6I6G). A) Bright field with iodine staining; B) Epifluorescence with Calcofluor and Texas Red staining. Black arrows: amylose precipitates; white arrows: inulin; gl: gluten aggregate.

Fig. 4. Viscosity profiles of rye porridge with different inulin and gluten proportions derived from measurement periods in the RVA. Control (—■—), 3:9 (··◆··), 6:6 (-▲-), 9:3 (—●—). Values are least square means ± standard errors. Different letters at specific time points indicate statistically significant differences between products ($P<0.05$).

Table 1. Conditions for the RVA test on the porridge samples (total duration 330 s)

Step	**1**	**2**	**3**	**4**	**5**
Temperature (°C)	75	75	75	75	75
Duration (s)	30	120	30	120	30
Agitation (rpm)	30	0	30	0	30

Figure 1

Click here to download high resolution image

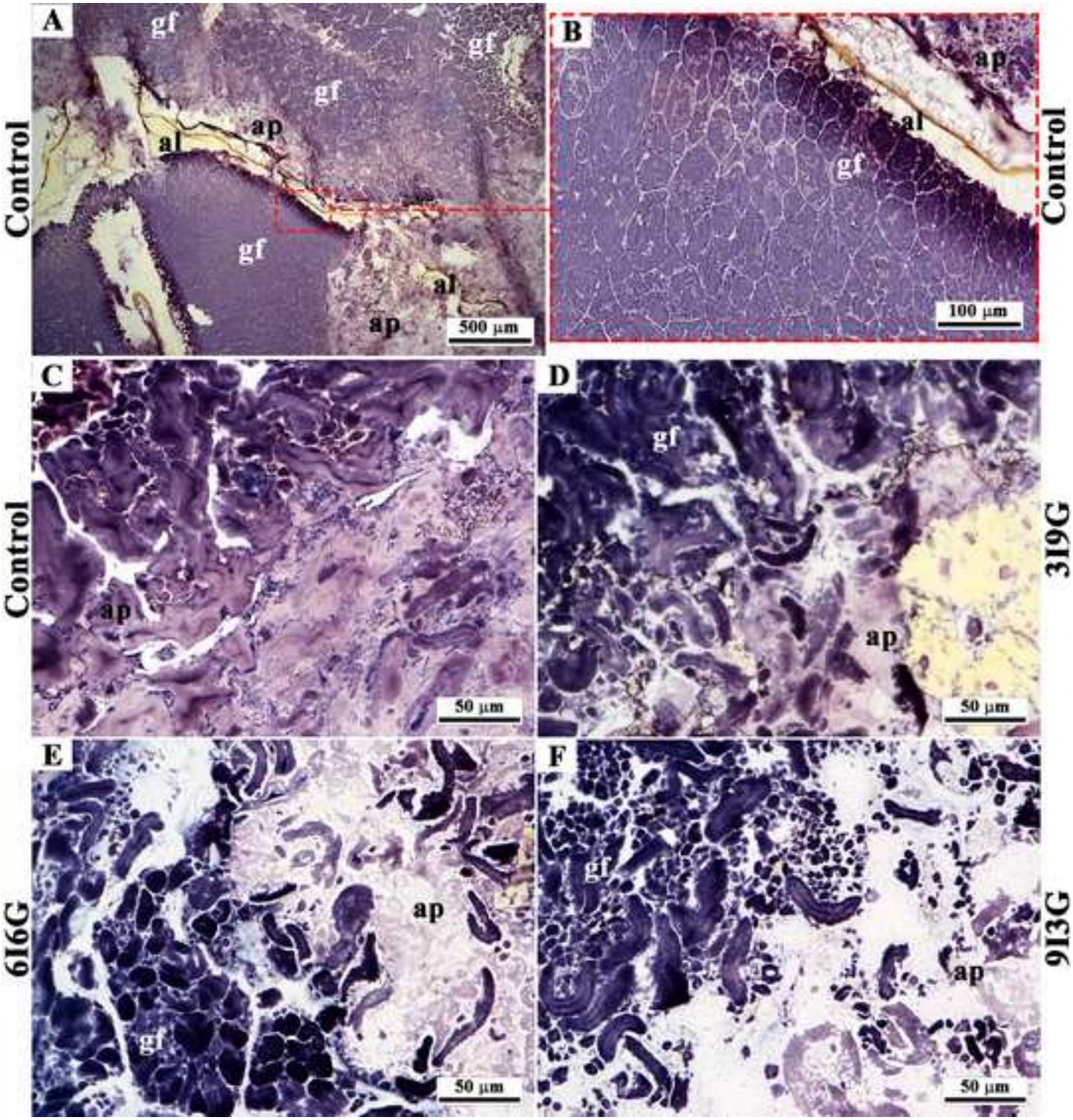

Figure 1 BW

Click here to download high resolution image

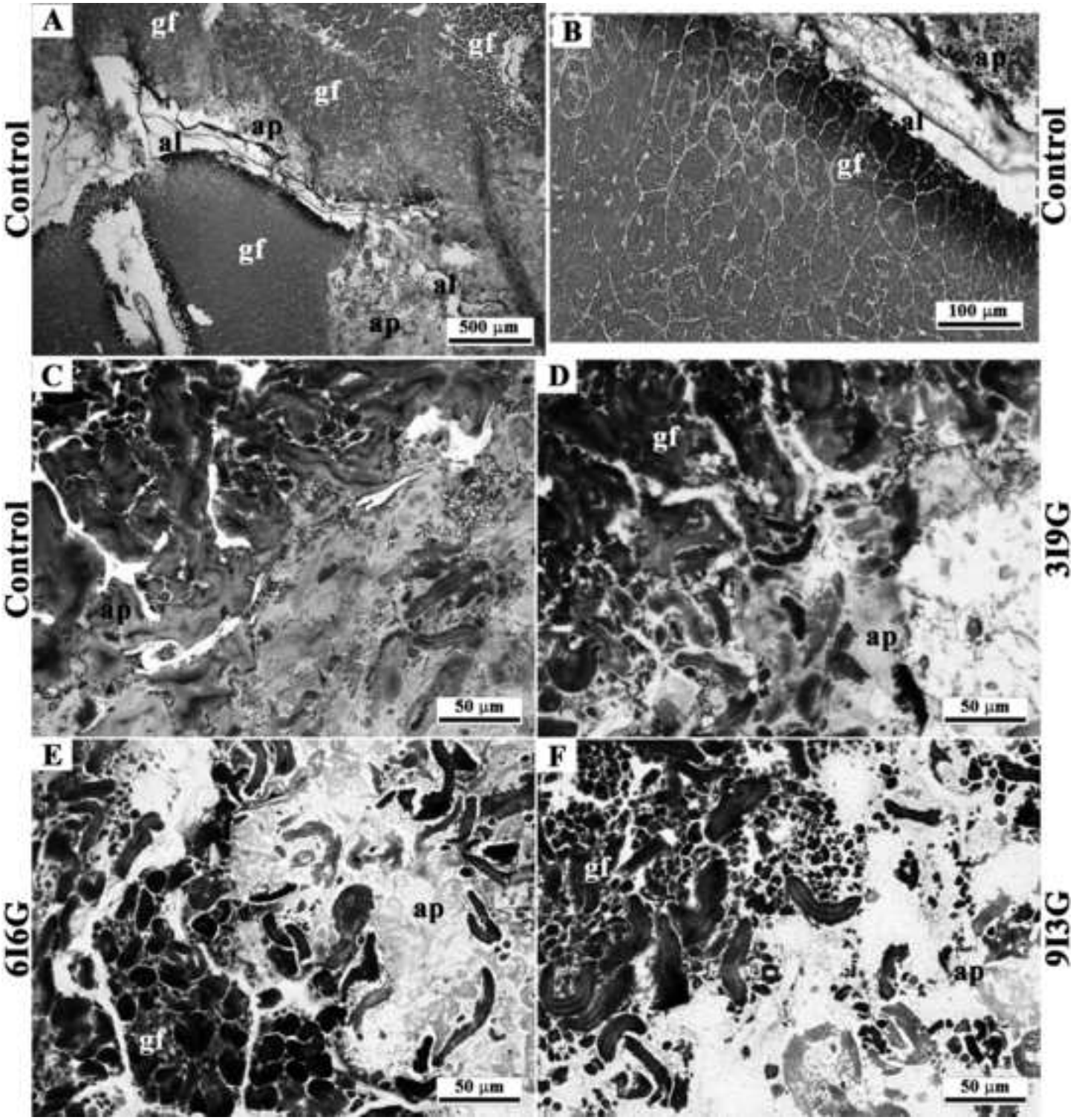

Figure 2

Click here to download high resolution image

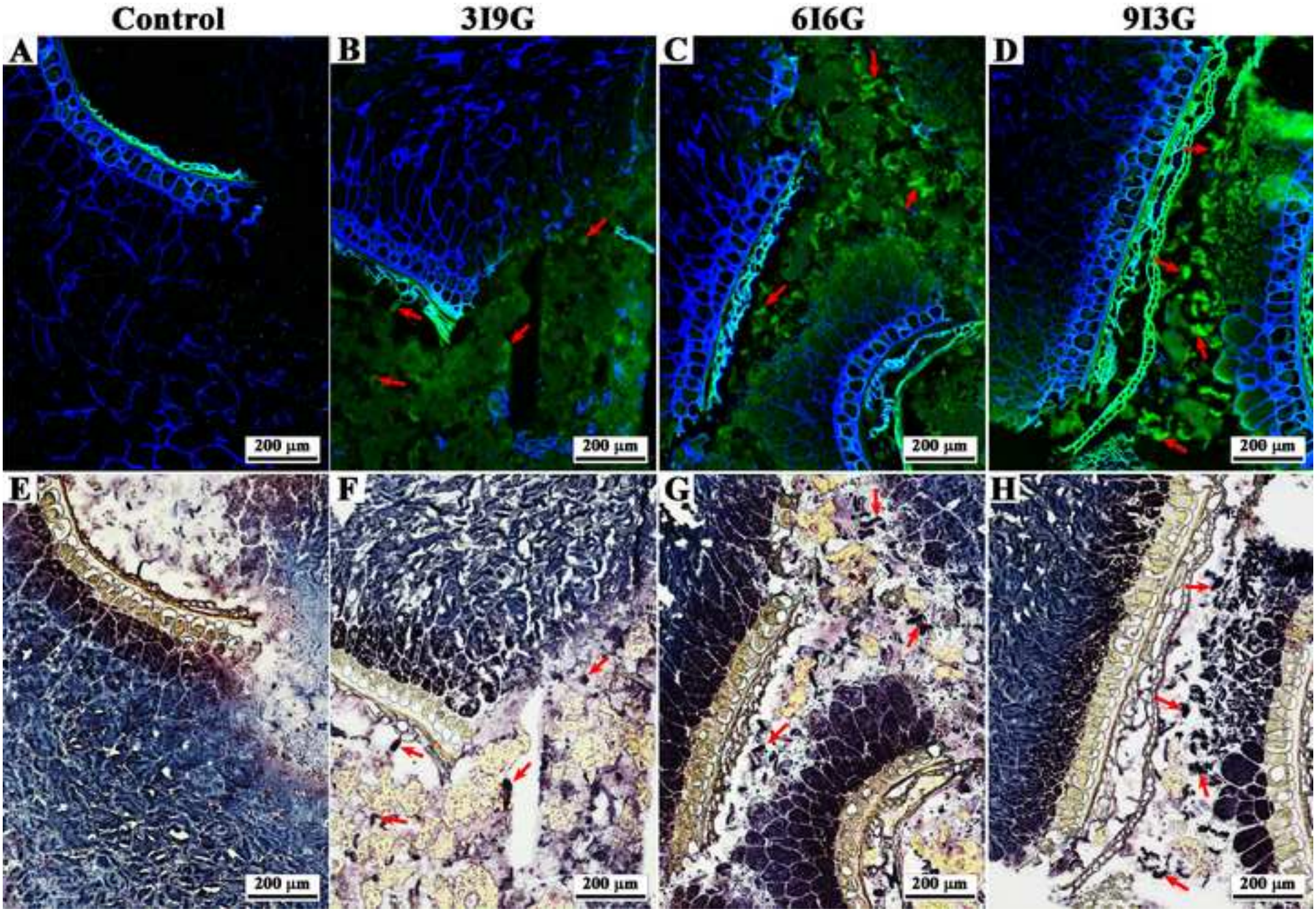

Figure 2 BW

Click here to download high resolution image

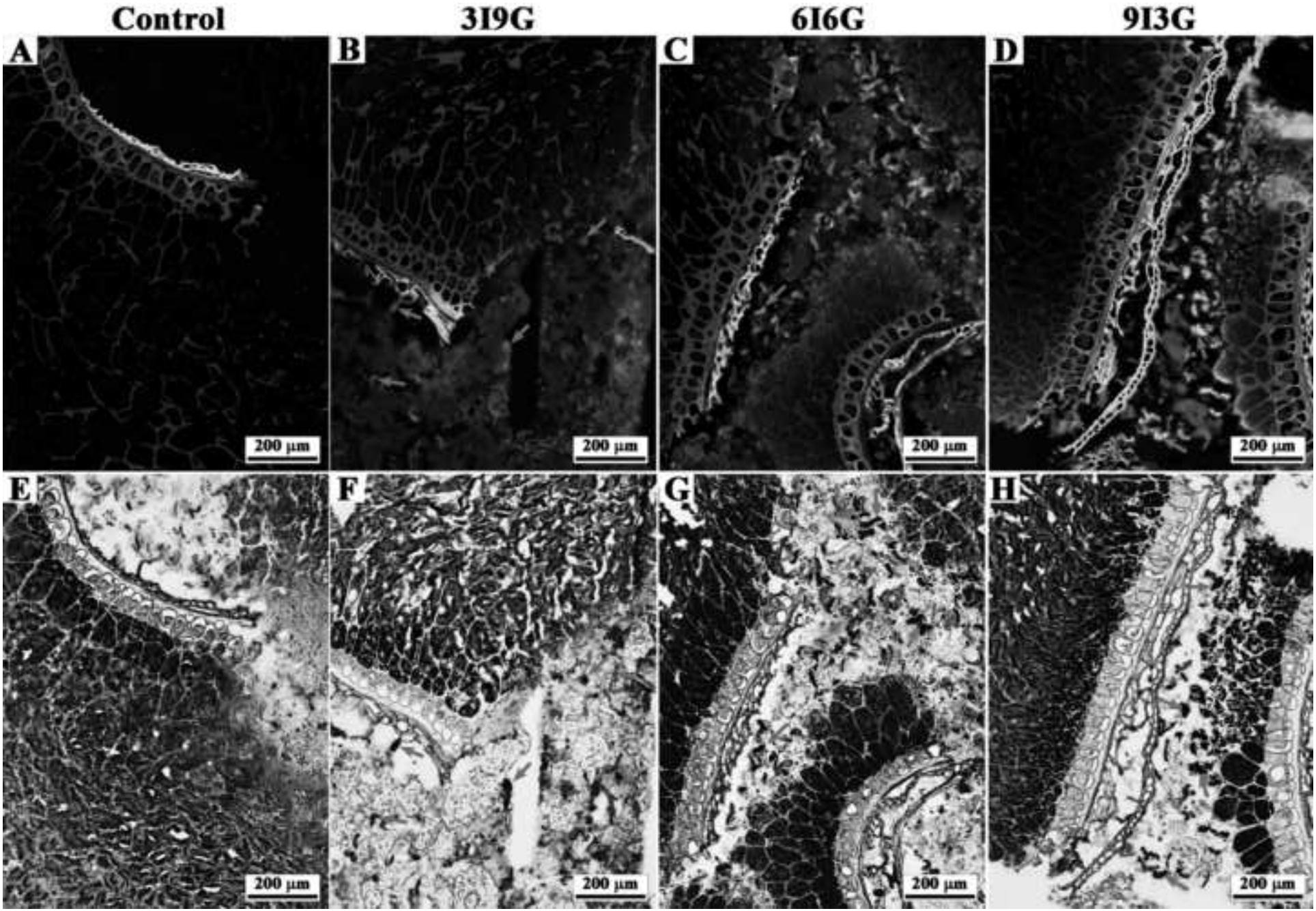

Figure 3

Click here to download high resolution image

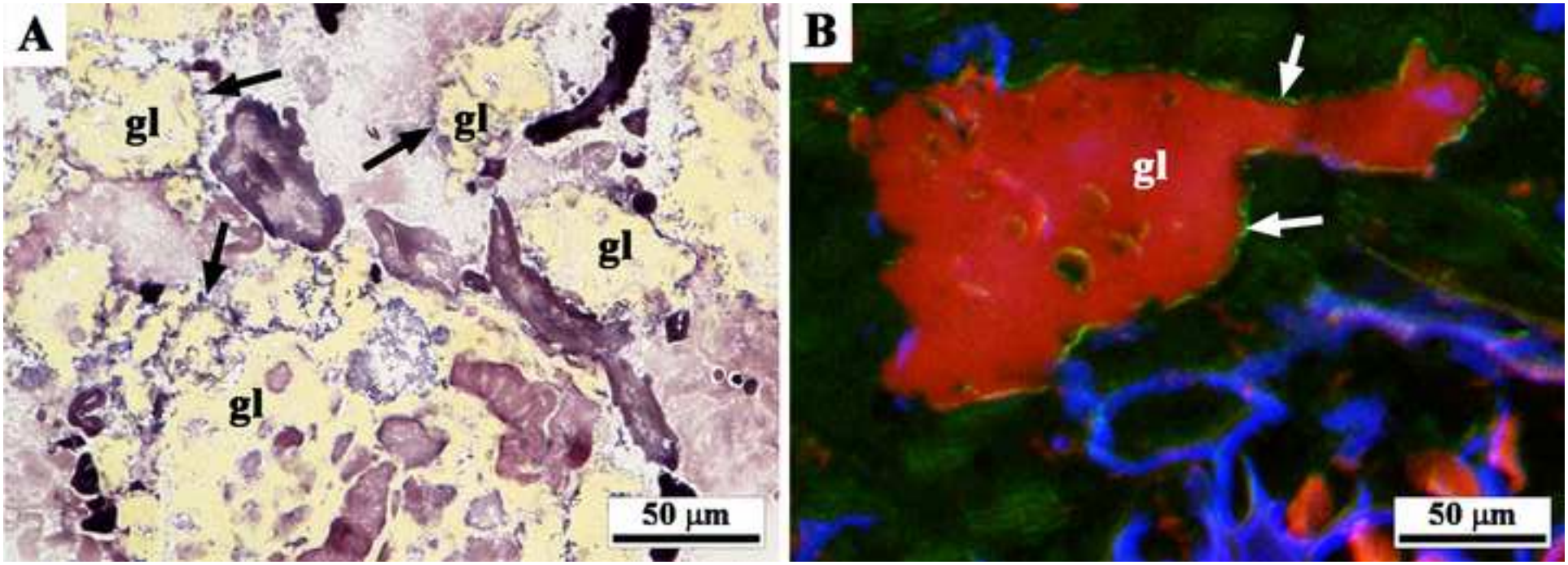

Figure 3 BW

Click here to download high resolution image

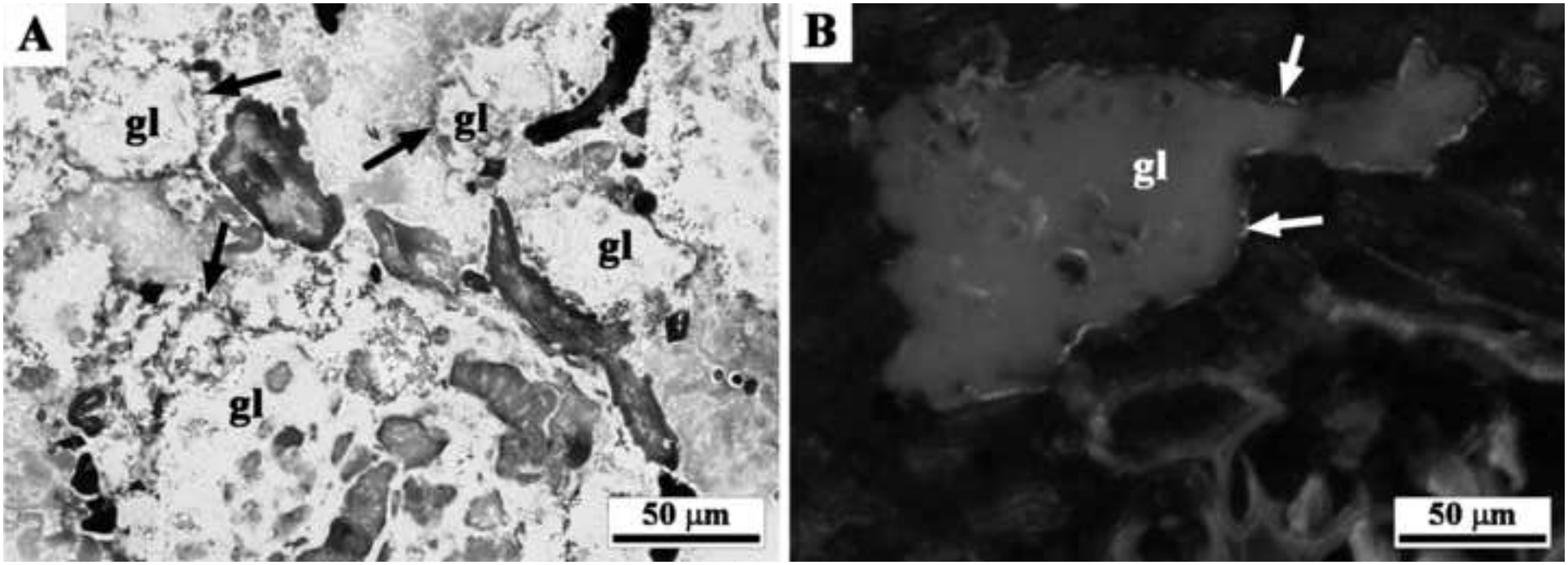

Figure 4

Click here to download high resolution image